UDC 539.53:546.302

**Y. Al-Khatatbeh*** (Amman, Jordan; New Haven, Connecticut, USA)
**K. K. M. Lee** (New Haven, Connecticut, USA)
**y.alkhatatbeh@psut.edu.jo*

# From superhard to hard: a review of transition metal dioxides $TiO_2$, $ZrO_2$, and $HfO_2$ hardness

*The high-pressure, high-temperature behavior of transition metal dioxides $TiO_2$, $ZrO_2$, and $HfO_2$ has been reviewed. In particular, early predictions and measurements that suggested superhard behavior for the transition metal dioxides have been considered. In subsequent studies, it has been concluded that superhardness is not intrinsic in the transition metal dioxides at ambient conditions or to phases produced at high-pressure and/or high-temperature conditions.*

***Keywords**: high-pressure transition metal dioxides, hardness, titanium dioxide, zirconium dioxide, hafnium dioxide.*

## INTRODUCTION

The high-pressure and/or high-temperature behavior of $TiO_2$, $ZrO_2$ and $HfO_2$ transition metal dioxides (TMDs) has attracted great interest over the past two decades because of their novel applications [1–49]. Their technological applications include the use in photocatalysis [50, 51], ceramics [52, 53], electronic storage media, and hydrogen storage applications [50, 54–57]. Therefore, because of their vast applications, there have been many studies investigating the mechanical [3, 4, 12, 40, 44, 49, 58, 59], optical [50, 60], and dielectric [50, 61] properties as well as their phase diagrams [1–39, 41–44, 46, 47]. In this review, we focus on the mechanical properties of the TMD phases formed at high-pressure and high-temperature conditions (see Fig. 1, Tables 1–3). In particular, we investigate the candidacy of these oxides as superhard materials based on relevant high-pressure studies.

For much of the last two decades, the highest-pressure phases of these dioxides were considered to be good candidates for superhard materials [10, 11, 14, 16, 17, 21, 25, 29, 31, 32, 62, 63]. That conclusion was largely formed in part by the assumption that the bulk modulus is a good indicator for the hardness. On the other hand, the shear modulus has been found to be a better estimator for the hardness [58, 64–66]. While these correlations have been evaluated for many compounds, the conclusion motivated researchers to test it for the TMDs [3, 4, 12, 40] (see lower). Although the hardness–shear modulus correlation was first concluded in 1998 [64], several studies since then [10, 11, 14, 16, 17, 21, 25, 29, 31, 32, 62, 63] assumed that the TMDs can possess superhard characteristics due to large bulk modulus values. However, more recent studies [3, 4, 12, 40] have brought doubt to this assumption and together with a few hardness measurements [67] and theoretical predictions [3, 4, 12, 40] conclude that these dioxides do not qualify as superhard.

This review is an effort to answer the question: Are there phases of $TiO_2$, $ZrO_2$ and $HfO_2$ that are superhard? To answer this question, we will introduce and

describe some aspects related to this topic. We will discuss the high-*p*, *T* synthesis route of superhard materials and discuss, in detail, early determinations on hardness of these dioxides, as well as recent conclusions. We will also investigate proxies for hardness with a comparison of the shear and bulk moduli and their correlation to the hardness of materials.

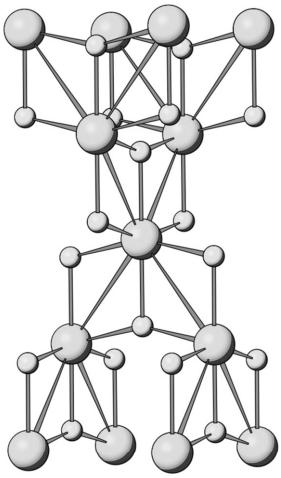

Phase: Anatase (AN)
Crystal structure: Tetragonal
Space group: $I4_1/amd$
Coordination number: 6
Observed in $TiO_2$

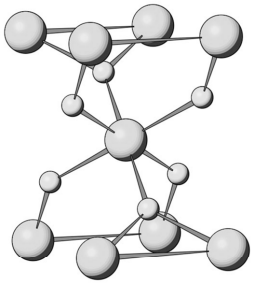

Phase: Rutile (RT)
Crystal structure: Tetragonal
Space group: $P4_2/mnm$
Coordination number: 6
Observed in $TiO_2$

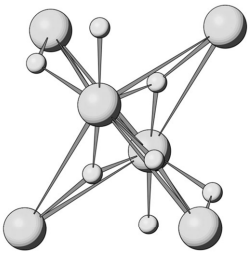

Phase: Columbite (CB)
Crystal structure: Orthorhombic
Space group: *Pbcn*
Coordination number: 6
Observed in $TiO_2$

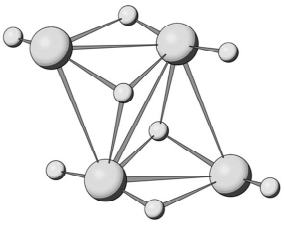

Phase: Baddelyite (MI)
Crystal structure: Monoclinic
Space group: $P2_1/c$
Coordination number: 7
Observed in $TiO_2$, $ZrO_2$, and $HfO_2$

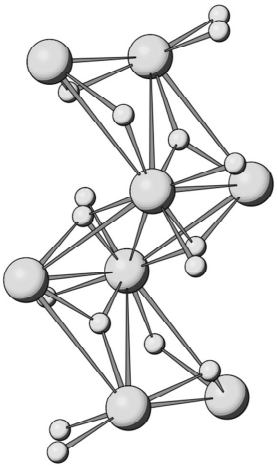

Phase: Orthorhombic I (OI)
Crystal structure: Orthorhombic
Space group: *Pbca*
Coordination number: 7
Observed in $TiO_2$, $ZrO_2$, and $HfO_2$

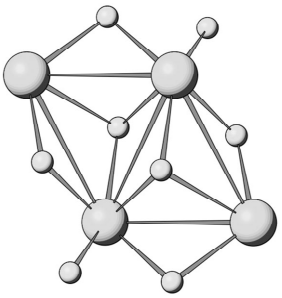

Phase: Orthorhombic II (OII)
Crystal structure: Orthorhombic
Space group: *Pnma*
Coordination number: 9
Observed in $TiO_2$, $ZrO_2$, and $HfO_2$

Fig. 1. Crystal structures and summary of the structural properties of observed phases of TMDs $TiO_2$, $ZrO_2$, and $HfO_2$. The larger spheres represent the transition metal Ti, Zr, or Hf cation, while the smaller spheres represent O.

**Table 1. Summary of the experimental equations of state of observed phases in TMDs $TiO_2$, $ZrO_2$, and $HfO_2$. 1σ uncertainties are given in parentheses. For values not available, NA is recorded**

| Phase | $TiO_2$ | | | | $ZrO_2$ | | | | $HfO_2$ | | | |
|---|---|---|---|---|---|---|---|---|---|---|---|---|
| | $V_0$, Å$^3$ | $K_0$, GPa | $K_0'$ | Ref. | $V_0$, Å$^3$ | $K_0$, GPa | $K_0'$ | Ref. | $V_0$, Å$^3$ | $K_0$, GPa | $K_0'$ | Ref. |
| AN | 34.08 (0.01) | 179 (2) | 4.5 (0.1) | [7] | – | – | – | – | – | – | – | – |
| BR | 32.26 (0.01) | 255 (10) | 4 (fixed) | [26] | – | – | – | – | – | – | – | – |
| RT | 31.20 (0.01) | 235 (10) | 4 (fixed) | [2] | – | – | – | – | – | – | – | – |
| | 31.25 (0.06) | 230 (20) | 6.6 (0.7) | [15] | | | | | | | | |
| | 31.20 (0.01) | 216 (2) | 7 (fixed) | [95] | | | | | | | | |
| CB | 30.53 (0.09) | 253 (12) | 4 (fixed) | [2] | – | – | – | – | – | – | – | – |
| | 30.59 (0.08) | 258 (8) | 4.1 (0.3) | [7] | | | | | | | | |
| MI | 28.06 (0.16) | 298 (21) | 4 (fixed) | [2] | 35.15 (0.03) | 210 (28) | 4 (fixed) | [3] | 34.50 (0.04) | 185 (23) | 4 (fixed) | [4] |
| | 28.06 (0.16) | 290 (10) | 4 (fixed) | [7] | 35.16 | 212 (24) | 8 (4) | [10] | 30.30 | 284 (30) | 5 (2) | [10] |
| | 28.06 (0.05) | 304 (6) | 3.9 (0.2) | [14] | 35.16 | 228 (10) | 4 (fixed) | [10]* | 30.30 | 325 (59) | 4 (fixed) | [10]* |
| | 27.62 (0.01) | 303 (5) | 3.9 (0.2) | [37] | 35.19 | 95 (8) | 4-5 | [23] | 34.67 | 145 (22) | 5 (fixed) | [24] |
| | 28.83 (0.07) | 175 (5) | 4 (fixed) | [28] | 35.06 | 187 | NA | [70] | 34.67 | 138 (52) | 4 (fixed) | [24]* |
| | | | | | 35.06 | 189 | NA | [71] | | | | |
| OI | 27.54 (0.13) | 314 (16) | 4 (fixed) | [2] | 33.65 (0.07) | 290 (11) | 4 (fixed) | [3] | 33.12 (0.13) | 266 (28) | 4 (fixed) | [4] |
| | 27.27 (0.02) | 318 (3) | 4 (fixed) | [13] | 33.49 | 243 (10) | 7 (2) | [10] | 28.93 | 281 (10) | 4.2 (0.9) | [10] |
| | 27.95 (0.17) | 222 (14) | 4 (fixed) | [28] | 33.49 | 380 (45) | 4 (fixed) | [10]* | 28.93 | 283 (11) | 4 (fixed) | [10]* |
| | | | | | 33.50 | 220 | 5 (fixed) | [23] | 33.11 | 210 (32) | 5 (fixed) | [24] |
| | | | | | | | | | 33.11 | 234 (37) | 4 (fixed) | [24]* |
| | | | | | | | | | 33.17 | 220 (10) | 4 (fixed) | [32] |

**Table 1. (Contd.)**

| | | | | | | | | | | | | |
|---|---|---|---|---|---|---|---|---|---|---|---|---|
| OII | 25.28 | 312 | 4 | [2] | 30.02 | 316 | 4 | [3] | 29.74 | 331 | 4 (fixed) | [4] |
| | (0.35) | (34) | (fixed) | | (0.11) | (27) | (fixed) | | (0.11) | (17) | | |
| | 26.27 | 431 | 1.35 | [14] | 30.81 | 444 | 1 | [10] | 26.54 | 340 | 2.6 | [10] |
| | (0.05) | (10) | (0.1) | | | (15) | (fixed) | | | (10) | (0.3) | |
| | 25.09 | 306 | 4 | [28] | 30.59 | 387 | 4 | [10]* | 26.54 | 304 | 4 (fixed) | [10]* |
| | (0.08) | (9) | (fixed) | | | (53) | (fixed) | | | (44) | | |
| | | | | | 30.22 | 332 | 2.30 | [16] | 29.65 | 312 | 4 (fixed) | [32] |
| | | | | | (0.02) | (8) | (0.40) | | | (10) | | |
| | | | | | 30.03 | 278 | 3.70 | [29] | | | | |
| | | | | | (0.08) | (11) | (0.22) | | | | | |
| | | | | | 30 | 265 | 4 | [31] | | | | |
| | | | | | | (10) | (fixed) | | | | | |

* Revised values to better compare results across studies; see [3, 4] for details.

**Table 2. Summary of the theoretical equations of state of observed phases in TMDs $TiO_2$, $ZrO_2$, and $HfO_2$. 1σ uncertainties are given in parentheses. For values not available, NA is recorded**

| Phase | $TiO_2$ | | | | $ZrO_2$ | | | | $HfO_2$ | | | |
|---|---|---|---|---|---|---|---|---|---|---|---|---|
| | $V_0$, Å$^3$ | $K_0$, GPa | $K_0'$ | Ref. | $V_0$, Å$^3$ | $K_0$, GPa | $K_0'$ | Ref. | $V_0$, Å$^3$ | $K_0$, GPa | $K_0'$ | Ref. |
| AN | 35.65 | 131 | 4 (fixed) | GGA | – | – | – | – | – | – | – | – |
| | (0.09) | (3) | | [2] | | | | | | | | |
| | 33.64 | 146 | 4 (fixed) | LDA | | | | | | | | |
| | (0.08) | (3) | | [2] | | | | | | | | |
| | 36.20 | 194 | NA | LCAO | | | | | | | | |
| | | | | [42] | | | | | | | | |
| | 33.70 | 195 | NA | LCAO- | | | | | | | | |
| | | (10) | | LDA [46] | | | | | | | | |
| RT | 32.18 | 216 | 4 (fixed) | GGA | – | – | – | – | – | – | – | – |
| | (0.02) | (2) | | [2] | | | | | | | | |
| | 31.89 | 215 | 5.35 | GGA | | | | | | | | |
| | (0.01) | (1) | (0.16) | [47] | | | | | | | | |
| | 30.47 | 250 | 4 (fixed) | LDA | | | | | | | | |
| | (0.01) | (2) | | [2] | | | | | | | | |
| | 33.10 | 243 | NA | LCAO | | | | | | | | |
| | | | | [42] | | | | | | | | |
| | 30.45 | 241 | NA | LCAO- | | | | | | | | |
| | | (10) | | LDA [46] | | | | | | | | |

**Table 2. (Contd.)**

| | | | | | | | | | | | | |
|---|---|---|---|---|---|---|---|---|---|---|---|---|
| CB | 31.75 (0.05) | 188 (4) | 4 (fixed) | GGA [2] | – | – | – | – | – | – | – | – |
| | 31.30 (0.15) | 250 (23) | 2.64 (0.70) | GGA [47] | | | | | | | | |
| | 29.97 (0.07) | 212 (9) | 4 (fixed) | LDA [2] | | | | | | | | |
| | 30.96 | 247 | NA | LCAO [42] | | | | | | | | |
| | 30.70 | 264 (10) | NA | LCAO-HF [46] | | | | | | | | |
| MI | 29.96 (0.04) | 157 (1) | 4 (fixed) | GGA [2] | 36.64 (0.04) | 143 (5) | 4 (fixed) | GGA [3] | 35.04 (0.04) | 168 (7) | 4 (fixed) | GGA [4] |
| | 28.01 (0.01) | 190 (2) | 4 (fixed) | LDA [2] | 35.62 | 138 | NA | GGA [63] | 34.81 | 152 | 4 (fixed) | GGA [19] |
| | 29.33 | 249 | NA | LCAO [42] | 36.19 | 137 | 4 (fixed) 4.12 | GGA [19] | 36.39 | 192 | 4 (fixed) | GGA [21] |
| | NA | 300 (10) | NA | LCAO-HF [46] | 36.00 | 218 | NA | GGA [39] | | | | |
| | | | | | 36.07 | 193 | | GGA [44] | | | | |
| | | | | | 34.55 (0.04) | 154 (8) | 4 (fixed) | LDA [3] | | | | |
| | | | | | 34.17 | 184 | 4 (fixed) | LDA [19] | | | | |
| | | | | | 35.63 | 157 | 2.38 | LDA [43] | | | | |
| OI | 28.71 (0.04) | 209 (2) | 4 (fixed) | GGA [2] | 35.14 (0.01) | 195 (2) | 4 (fixed) NA | GGA [3] | 33.58 (0.01) | 218 (2) | 4 (fixed) | GGA [4] |
| | 27.02 (0.04) | 236 (3) | 4 (fixed) | LDA [2] | 34.13 | 227 | | GGA [63] | 33.53 | 197 | 4 (fixed) | GGA [19] |
| | 28.31 (0.06) | 272 (9) | 3.38 (0.19) | B3LYP [47] | 34.69 | 204 | 4 (fixed) 4.23 | GGA [19] | 35.04 | 221 | 4 (fixed) | GGA [21] |
| | | | | | 34.40 | 230 | NA | GGA [39] | | | | |
| | | | | | 34.50 | 210 | | GGA [44] | | | | |
| | | | | | 33.33 (0.02) | 214 (4) | 4 (fixed) | LDA [3] | | | | |
| | | | | | 32.97 | 236 | 4 (fixed) | LDA [19] | | | | |
| | | | | | 31.73 | 272 | 4.63 | LDA [43] | | | | |

**Table 2. (Contd.)**

| | | | | | | | | | | | | |
|---|---|---|---|---|---|---|---|---|---|---|---|---|
| OII | 25.97 | 261 | 4 (fixed) | GGA | 31.35 | 251 | 4 (fixed) | GGA | 30.12 | 260 | 4 (fixed) | GGA |
| | (0.10) | (7) | | [2] | (0.04) | (3) | | [3] | (0.05) | (4) | | [4] |
| | 25.38 | 281 | 4.8 | GGA | 30.46 | 234 | NA | GGA | 31.86 | 251 | 4 (fixed) | GGA |
| | | | | [49] | | | | [63] | | | | [19] |
| | 24.44 | 300 | 4 (fixed) | LDA [2] | 30.86 | 251 | 4 (fixed) | GGA | 29.75 | 259 | 4 (fixed) | GGA |
| | (0.04) | (6) | 4.57 | | | | | [19] | | | | [21] |
| | 26.14 | 306 | 3.85 | LDA [11] | 30.80 | 254 | 4.11 | GGA | | | | |
| | | | | | | | | [39] | | | | |
| | 23.81 | 341 | NA | LDA [49] | 30.94 | 213 | NA | GGA | | | | |
| | | | | | | | | [44] | | | | |
| | NA | 380 | | LCAO-HF | 29.70 | 289 | 4 (fixed) | LDA | | | | |
| | | (10) | | [46] | (0.02) | (3) | | [3] | | | | |
| | | | | | 29.24 | 298 | 4 (fixed) | LDA | | | | |
| | | | | | | | | [19] | | | | |
| | | | | | 29.41 | 305 | 4.68 | LDA | | | | |
| | | | | | | | | [43] | | | | |

**Table 3. Summary of the volume change across OI → OII phase transition in TMDs $TiO_2$, $ZrO_2$, and $HfO_2$**

| Dioxide | Volume change across OI → OII phase transition, % | | | |
|---|---|---|---|---|
| | Experiment | Ref. | Theory | Ref. |
| $TiO_2$ | 8.3 | [2] | 7.6 (GGA) | [2] |
| | 2.6 | [13, 14] | 8.2 (LDA) | [2] |
| | 7.4 | [28] | | |
| $ZrO_2$ | 10 | [3] | 9.9 (GGA) | [3] |
| | 5.8 | [10] | 10.5 (GGA) | [19] |
| | 9 | [31] | 10.6 (LDA) | [3] |
| $HfO_2$ | 8.6 | [4] | 9.5 (GGA) | [4] |
| | 7.4 | [10] | 9.9 (GGA) | [19] |
| | 8 | [32] | 10.4 (LDA) | [19] |

**Superhard versus hard materials**

A material is defined as superhard if its hardness exceeds 40 GPa using a Vickers hardness test (e.g., [68]) which, like all hardness tests, observes a material's ability to resist plastic deformation from a standard indenter. However, depending on chemical bonding (i.e., metallic, covalent, and ionic, respectively), the materials can be classified into three types according to their hardness [69]: (1) borides, carbides, and nitrides formed with transition metals, such as TiN, WC and $TiB_2$; (2) borides, carbides, and nitrides of Al, Si, and B, as well as diamond; and (3) oxides of Al, Zr, Ti, and Be. Materials that consist of elements from the B–C–N triangle are among the hardest materials [68]; examples include diamond, cubic boron nitride (cBN), $C_3N_4$, $BC_2N$, and $B_4C$. It is important to note that although materials of hardness lower than 40 GPa are not superhard, they can still be called

hard materials, and are still of industrial importance and interest, if they show a hardness value > ~ 15 GPa (e.g., [68]).

### Elasticity

The stresses and strains inside a continuous elastic material can be described by a linear relationship mathematically similar to Hooke's Law (i.e., $F = -kx$). However, the strain state in a solid medium around a point cannot be described by a single vector due to the added complexity of being able to be compressed, stretched, and sheared at the same time, along different directions. To do so, the stresses at that point can be at once pushing, pulling, and shearing. To capture this complexity, the relevant state of the medium around a point is represented by two second-order tensors, the strain tensor ε (in place of the displacement $x$) and the stress tensor σ (replacing the restoring force $F$). Thus, the Hooke's spring law for continuous media is then:

$$\sigma_{ij} = \sum_{kl} c_{ijkl} \varepsilon_{kl} \,, \tag{1}$$

where $c_{ijkl}$ is the fourth-order elasticity tensor (replacing the spring constant $k$), represented by 81 (i.e., $3^4$) $c_{ijkl}$ values.

Due to symmetry and for simplicity, Voigt notation is used and is represented by reducing its order: *xx, yy, zz, yz, xz, xy* components are replaced by 1, 2, 3, 4, 5, 6, respectively, and then Equation (1) is reduced to [49]:

$$\sigma_i = c_{ij} \varepsilon_j \,, \tag{2}$$

where $c_{ij}$ is the elastic constants matrix, which is also symmetric, and the latter equation can be rewritten as:

$$\begin{bmatrix} \sigma_1 \\ \sigma_2 \\ \sigma_3 \\ \sigma_4 \\ \sigma_5 \\ \sigma_6 \end{bmatrix} = \begin{bmatrix} c_{11} & c_{12} & c_{13} & c_{14} & c_{15} & c_{16} \\ & c_{22} & c_{23} & c_{24} & c_{25} & c_{26} \\ & & c_{33} & c_{34} & c_{35} & c_{36} \\ & & & c_{44} & c_{45} & c_{46} \\ & & & & c_{55} & c_{56} \\ & & & & & c_{66} \end{bmatrix} \cdot \begin{bmatrix} \varepsilon_1 \\ \varepsilon_2 \\ \varepsilon_3 \\ \varepsilon_4 \\ \varepsilon_5 \\ \varepsilon_6 \end{bmatrix} . \tag{3}$$

Due to the inherent symmetries of ε, σ, and $c$, only 21 elastic coefficients of the latter are independent. For isotropic media, $c$ can be reduced to only two independent numbers, the bulk modulus $K$ and the shear modulus μ, that quantify the material's resistance to changes in volume and to shearing deformations, respectively (see below).

### Compressibility and equation of state

The compressibility, β, of a solid is simply the relative change of the volume, $V$, of a material due to an applied pressure, $p$. The bulk modulus, $K$, or the inverse of compressibility, is often used in the literature and at isothermal conditions; the isothermal bulk modulus ($K_T$) is defined as at constant temperature $T$:

$$K_T = -V\left(\frac{\partial p}{\partial V}\right)_T . \tag{4}$$

More compressible materials have smaller bulk moduli, whereas less compressible materials have high bulk moduli.

The bulk modulus is one of the most important parameters of the equation of state as it is a measure of how much a material compresses under stress. The bulk modulus can be measured in a variety of ways, including through ultrasonic and Brillouin scattering measurements (e.g., [70–72]) as well as by using powder X-ray diffraction (e.g., [2–4, 29, 41]), such that using these data one can easily measure the volume at various pressures and thus construct the pressure–volume curve needed to obtain the bulk modulus.

In general, the equation of state (EOS) is defined as a relationship between thermodynamic parameters such as pressure, temperature, volume, and internal energy of the material. There are many EOSs, however, for most solid materials, the Birch-Murnaghan [73] EOS is among the most widely used for pressures up to a few 100 GPa [74]. The Birch-Murnaghan EOS is given as

$$p(V) = 3K_0 f(1+2f)^{\frac{5}{2}}(1 + af + bf^2 + ...), \quad (5)$$

where

$$f = \frac{1}{2}\left[\left(\frac{V}{V_0}\right)^{-\frac{2}{3}} - 1\right],\ a = \frac{3}{2}(K_0' - 4), \text{ and } b = \frac{3}{2}K_0K_0'' + \frac{3}{2}K_0'(K_0' - 7) + \frac{143}{6}. \quad (6)$$

Equation (5) can be truncated for the terms $f^2$ and above yielding the 3rd-order Birch-Murnaghan EOS, which can be rewritten such that there are only three parameters to describe the EOS: the zero-pressure volume ($V_0$), the bulk modulus at zero pressure ($K_0$), and the first pressure derivative of the bulk modulus at zero pressure ($K_0'$):

$$p(V) = \frac{3K_0}{2}\left[\left(\frac{V}{V_0}\right)^{-\frac{7}{3}} - \left(\frac{V}{V_0}\right)^{-\frac{5}{3}}\right]\left\{1 + \frac{3}{4}(K_0' - 4)\left[\left(\frac{V}{V_0}\right)^{-\frac{2}{3}} - 1\right]\right\}. \quad (7)$$

In fact, it is important here to emphasize the sensitivity of the bulk modulus to the other parameters, $V_0$ and $K_0'$. For example, a small change in $V_0$ can result in a large change in $K_0$ [41]. However, $V_0$ is generally known for a material (if it is stable and/or quenchable at zero-pressure it can be measured), although there are many materials/phases that are not quenchable to zero pressure, and thus is estimated or is fit as a free parameter in the EOS using the $G$ vs. $g$ formalism [75]. This is of particular importance in the case of $TiO_2$, where the high-pressure phase OII is not stable at ambient conditions and thus its $V_0$ can not be measured, and its $V_0$ has been extrapolated or fit [2], although an earlier work claimed quenching that phase to zero pressure at cryogenic temperatures [14]. On the other hand, unlike $V_0$ (usually a measured value), $K_0'$ is a parameter determined from the EOS fit. For a given set of data, values of $K_0' < 4$ (> 4), a higher (lower) $K_0$ value is obtained; however, since most materials have $3 \le K_0' \le 6$ [74, 76], it is commonplace to fix $K_0'$ to 4 [2–4, 41] and thus use a truncated 2nd-order-Birch-Murnaghan EOS, where the higher-order terms are ignored from Equation (5) such that Equation (7) becomes

$$p(V) = \frac{3K_0}{2}\left[\left(\frac{V}{V_0}\right)^{-\frac{7}{3}} - \left(\frac{V}{V_0}\right)^{-\frac{5}{3}}\right]. \quad (8)$$

For example in the case of OII-$TiO_2$ phase, an earlier study [14] found $K_0$ = 431 GPa at $K_0' = 1.35$; however, a later study [2] found that this value is noticeably reduced to 358 GPa when $K_0'$ is fixed to a value of 4 (see Table 1). Thus for a more reliable comparison of properties between materials, it is necessary to compare the bulk moduli of the same material/phase at the same $K_0'$ and $V_0$ values.

In any event, the implicit assumption that the bulk modulus is a suitable proxy for the mechanical strength of a material has been examined [58, 64–66]. This assumption has been evaluated by others and applied for different materials including TMD and will be discussed further [3, 4, 58].

**Shear modulus**

The shear modulus (μ) of a material can be defined as the ratio of its shear stress to the shear strain. The individual elastic constants ($c_{ij}$'s) are often used to obtain the shear modulus of the material. For example, for an orthorhombic material, the Voigt shear modulus is defined as [49]:

$$15\mu_V = (c_{11} + c_{22} + c_{33}) - (c_{12} + c_{13} + c_{23}) + 3(c_{44} + c_{55} + c_{66}). \quad (9)$$

The main method of measuring μ is by acoustical methods, namely ultrasonic or Brillouin scattering. With these methods, the acoustic velocities are measured. Using the known density of the material and its geometry, it is trivial to compute both the bulk and shear moduli as they are related to the bulk sound, compressional, and shear velocities, $v_B$, $v_p$ and $v_s$:

$$\begin{aligned} \nu_B &= \sqrt{\frac{K}{\rho}}; \\ \nu_p &= \sqrt{\frac{\frac{4}{3}K + \mu}{\rho}}; \\ \nu_s &= \sqrt{\frac{\mu}{\rho}}. \end{aligned} \quad (10)$$

These measurements can additionally be conducted at high pressures in order to measure the pressure derivatives of both $K$ and μ. These methods are not used as widely as X-ray diffraction, in which the shear modulus cannot be measured or inferred, and as such there are fewer measurements of shear moduli as compared to bulk moduli.

Similar to assumptions regarding the bulk modulus and hardness correlations, the shear modulus has been assumed as a suitable proxy for the strength of materials [58, 64–66] and, thus, has been often used as an indicator for their hardness. This assumption has also been evaluated for TMDs [3, 4].

**Hardness versus bulk modulus and shear modulus**

It is important to mention that both bulk and shear moduli are elastic quantities, whereas the hardness is a plastic quantity and, thus, there is no direct relationship that relates shear and bulk moduli to hardness. However, indenting a material (e.g.,

to measure its hardness), is likely a subject to more shearing effort than compressing. Despite the lack of a direct relationship between elastic moduli and hardness, several studies have tried to use the moduli as hardness proxies. In Fig. 2, we show a compilation of hardness values versus bulk and shear moduli. In this compilation, we find a strong positive correlation between hardness and shear modulus, whereas the hardness relationship with bulk modulus is tenuous. We note that pure metals do not necessarily follow these trends; for instance, rhenium and tungsten do not follow the hardness–shear modulus correlation (see Fig. 2).

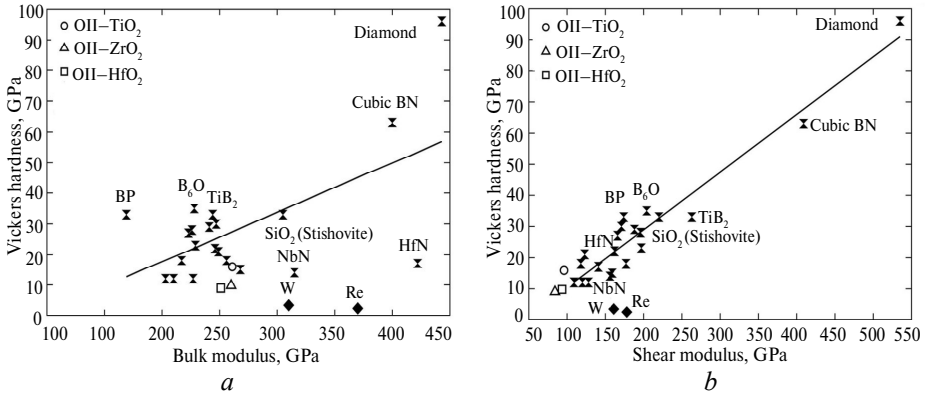


Fig. 2. Hardness versus bulk (*a*) or shear (*b*) moduli for a variety of materials. Figure adopted from Teter [64] where experimental moduli and hardness values are depicted. Solid symbols are shown for ionic and covalent compounds (vertical bowties), and pure metals (diamonds). Open symbols are shown for the OII phase of $TiO_2$ (circles), $ZrO_2$ (triangles) and $HfO_2$ (squares). The computed hardness values are given for $ZrO_2$ [3] and $HfO_2$ [4]. The solid line is a best fit to existing data. The calculated hardness of $TiO_2$ [40] is plotted against the calculated bulk [2] and shear moduli [49]. Error bars and some of the compound names were left out for clarity.

## HIGH-*p*, *T* SYNTHESIS ROUTE OF SUPERHARD MATERIALS

Superhard materials have been synthesized in many ways including: chemical reaction (e.g., $ReB_2$ [77]), high temperatures (e.g., CVD diamond [78]), high pressures (e.g., M-carbon [79]), and simultaneous high pressures and high temperatures (e.g., diamond and c-$Si_3N_4$ [80]). Here we focus on methods, which incorporate the use of simultaneous high-*p*, *T* techniques to transform materials into superhard materials. The most popular example of a superhard material is diamond, and while diamond is produced in nature, it is due to the high pressures and high temperatures within the deep Earth that turns graphite into this relatively stable, yet metastable phase (e.g., [81]). This transformation, from an abundant and relatively soft material into a rare and superhard material, has attracted researchers to find ways to synthesize other superhard materials.

In general, the basic assumption is that the hardness of a material increases as its molar volume decreases, either within a single phase, or across volume-reducing phase transitions [82]. As a result, quenchable high-pressure phases provide a promising route for the synthesis of mechanically stronger materials [80, 83]. Therefore, this successful route has attracted researchers to apply it to the TMDs in an effort to produce hard high-pressure phases [3, 4, 12].

## TRANSITION METAL DIOXIDES $TiO_2$, $ZrO_2$ AND $HfO_2$

### Observed phases

Figure 1 summarizes the experimentally observed phases for each dioxide. We note that the intermediate-pressure phase baddeleyite (MI) in $TiO_2$ is the ambient-pressure structure in the case of $ZrO_2$ and $HfO_2$. We also note that the coordination number increases for high-pressure phases, as expected. Additionally, for the case of $TiO_2$, there are three phases found at ambient conditions: brookite (rare polymorph [26]) and anatase are stable phases, whereas rutile (RT) is a metastable phase formed at high temperatures. Additionally, there are other observed phases at high temperature for $ZrO_2$ and $HfO_2$: tetragonal [84, 85] and cubic [86, 87] phases. It is also important to note that as the pressure increases, there is no trend of increasing or decreasing in structural symmetry. For instance, rutile (tetragonal) transforms to a lower symmetry (monoclinic MI) and then to a higher symmetry (orthorhombic OI). However, one should expect that the density increases for high-pressure phases and this change may be significant for a large change in the coordination number, i.e., OI → OII transition (see lower) (Fig. 3).

### Review of previous high-pressure/temperature studies

The high-$p$, $T$ behavior of TMDs $TiO_2$, $ZrO_2$, and $HfO_2$ has been experimentally explored mostly using both X-ray diffraction (XRD) technique [1–4, 6, 7, 9, 10, 13–16, 22–24, 26–36, 38, 48, 88, 89] and Raman spectroscopy measurements [5, 6, 17, 20, 45, 84, 90–93]. On the other hand there are many theoretical studies on the high-pressure investigations of these dioxides, most of them using density-functional theory (DFT) based on first-principles computations [2–4, 11, 19, 21, 39, 42–44, 46, 47, 49, 63] (see Tables 1 and 2). Generally, measurements and calculations of the EOS of TMDs $TiO_2$, $ZrO_2$ and $HfO_2$ are in good agreement. The major goal of several studies was to investigate the equation of state and phase diagram under high temperatures and/or high pressures, and the hardness of resulting quenched phases [2–4, 7, 10, 13–16, 23, 24, 26–32, 37, 38, 67, 94, 95].

### Density nature of OII phase: volume change across OI → OII transition

The coordination number across OI → OII phase transition increases from 7 to 9 (see Fig. 2), and, thus, this relatively large increase in coordination suggests a large change in density (~ 10%) as well. Previous measurements on TMDs $ZrO_2$ and $HfO_2$ have observed this large change and obtained comparable results (see Fig. 2, Table 3) [3, 4, 10, 31, 32]. Therefore, in both earlier [10, 31, 32] and recent studies [3, 4], the high-density nature of the OII has been concluded for $ZrO_2$ and $HfO_2$.

However, until recently, this was not the case for $TiO_2$. Early measurements on $TiO_2$ [13, 14] found a relatively small increase in density (~ 2.6%) in the OI → OII transition, in contrast with the same transition in $ZrO_2$ and $HfO_2$ (~ 10%) (see Table 3) [3, 4, 10, 31, 32]. In addition, this value (2.6%) is much lower than the predicted value for $TiO_2$ and similar dioxides using DFT calculations (see Table 3) [3, 4, 19]. However, later studies on $TiO_2$ confirmed the high-density nature of the OII phase using both experiment [2, 28] and theory [2] and showed good agreement of the volume change across OI → OII phase transition of $TiO_2$ in comparison to similar dioxides including $ZrO_2$ and $HfO_2$ (see Table 3).

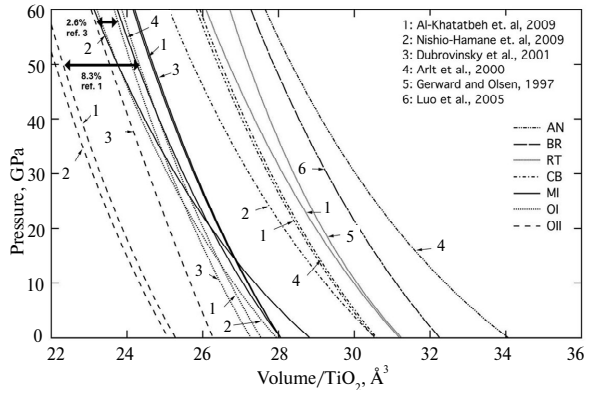


*a*

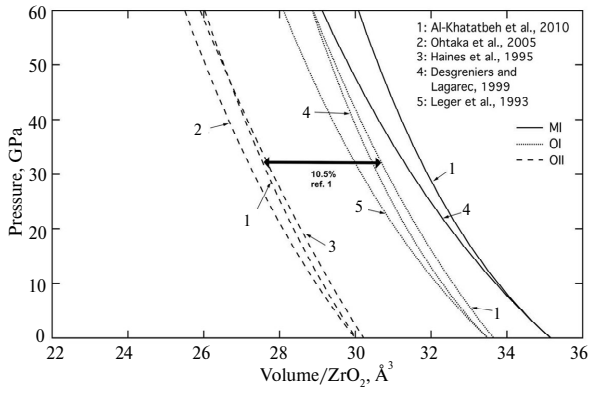


*b*

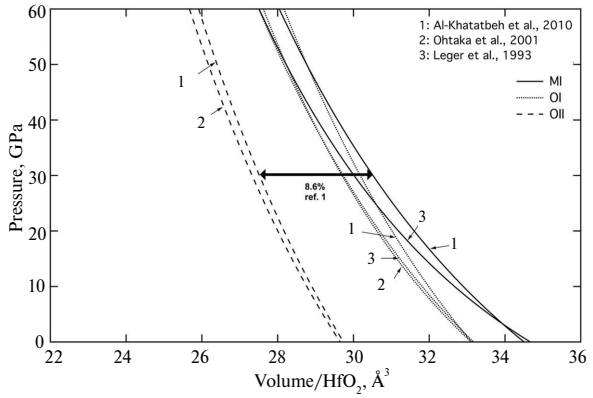


*c*

Fig. 3. Experimental pressure-versus-volume curves for the phases for one formula unit of TMDs $TiO_2$ (*a*), $ZrO_2$ (*b*), and $HfO_2$ (*c*) as observed in various studies [2, 7, 10, 13–16, 23, 24, 26, 29, 32]. The large volume collapse across OI → OII transition is shown.

## Stability of OII phase

Experiments have concluded that the OII phase is the most stable phase at high pressure: up to ~ 70, 100 and 105 GPa for $TiO_2$ [28], $ZrO_2$ [29], and $HfO_2$ [4], respectively. However, there are two main differences when one compares $TiO_2$ to both $ZrO_2$ and $HfO_2$. First, in $TiO_2$ the synthesis conditions for OII requires both high pressure and high temperature [2, 14, 28], whereas in the case of $ZrO_2$ and $HfO_2$, temperature is not required, although it facilitates the phase transition and reduces the deviatoric stress [3, 4, 29, 32]. Second, it has been observed that this

phase is quenchable to room conditions only for $ZrO_2$ and $HfO_2$ [3, 4, 29, 32], whereas it is stable only at room temperatures at high pressures for $TiO_2$ [2, 14, 28]. We also note that a recent study [9] has found evidence for a post-OII phase ($Fe_2P$-type structure) of $TiO_2$ that is predicted to be slightly denser than OII.

## CANDIDACY OF TMD PHASES TO BE SUPERHARD MATERIALS

In this section, we discuss whether the TMDs $TiO_2$, $ZrO_2$, and $HfO_2$ are good candidates for superhard materials by reviewing previous measurements and calculations made on the hardness of these dioxides. We also examine the correlation of hardness with both bulk and shear moduli (see Fig. 2).

While these two correlations have been evaluated for many compounds (see Fig. 2), the conclusion has motivated researchers [3, 4, 12] to test it for the case of TMDs $TiO_2$, $ZrO_2$, and $HfO_2$.

### Measurements made on hardness of high-*p* TMDs

The hardness of a quenched OII-$TiO_2$ sample has been measured to be 38 GPa at cryogenic temperatures [14]. This high hardness value coupled with the high bulk modulus of 431 GPa suggested that this phase could be superhard, despite $K$ not being a reliable proxy for hardness. Even so, as discussed above, the bulk modulus of that phase is not so high if $K_0'$ is constrained to 4 (i.e., 431 GPa versus 358 GPa). Additionally, later theoretical studies have shown that the hardness of OII-$TiO_2$ is expected to have a much lower value (see below). This is consistent with the low shear modulus that has been calculated [49]. Thus, it is unlikely that quenched OII-$TiO_2$ is superhard.

For both $ZrO_2$ and $HfO_2$, experimental observations of the hardness were regarded as low and scattered (11–17 GPa for $ZrO_2$ and 6–13 GPa for $HfO_2$) due to poor sintering [67]. However, this is likely a reflection of the low intrinsic hardness of this phase rather than related to a sample preparation.

### Calculations made on hardness of high-*p* TMDs

Simunek and Vackar proposed a scaling model to estimate the mechanical strength of covalent and ionic compounds [96] that has been used subsequently for the TMD phases. In this model, hardness increases with increasing average number of bonds per atom, decreasing average atomic volume, smaller coordination number, and shorter average bond length [96]. In addition to crystal chemistry, the hardness depends also on the characteristic length scale ($R$i) of the charge density distribution about each atom. Using this model, Ding et al. [12], have estimated the hardness of OII-$TiO_2$ to be ~ 26 and ~ 20 GPa for the recently observed $Fe_2P$-type-$TiO_2$ phase [9]. Additional evidence of the non-superhard candidacy of OII-$TiO_2$ has been recently introduced [40]. Their calculations on OII-$TiO_2$, using another scaling model based on the electronegativities and covalent radii of the constituent atoms as well as the bond lengths between atoms, have predicted a hardness value of ~ 16 GPa (see Fig. 2), less than half the earlier measured value of 38 GPa [14]. These results are also in agreement with the shear modulus–hardness correlation (see Fig. 2) [58, 64–66].

Al-Khatatbeh et al. [3, 4] have also used the Simunek and Vackar scaling model [96] to estimate the mechanical strength of the experimentally observed ambient temperature of $ZrO_2$ and $HfO_2$ phases. In summary, these studies have concluded that all phases, MI, OI, and the highest-pressure phase OII, do not qualify as superhard candidates with a hardness value of ~ 10 GPa only (see Fig. 2). They have [3, 4] also concluded that the shear modulus correlates much better with the

hardness than the bulk modulus in agreement with previous conclusions for other compounds (see Fig. 2) [58, 64–66].

## CONCLUSIONS

In this review we conclude that the high-pressure phases of TMDs $TiO_2$, $ZrO_2$, and $HfO_2$ are hard materials, rather than good superhard candidate materials as their hardness is much lower than 40 GPa, a prerequisite for a material to be superhard. While it has been also concluded that the shear modulus is a better estimator for the hardness than the bulk modulus, further experimental studies are still needed to measure the shear modulus and hardness in order to confirm the shear modulus–hardness correlation for the high-pressure phases of TMDs $TiO_2$, $ZrO_2$, and $HfO_2$ that have been predicted. Additionally, we have concluded that the current high-pressure synthesis route has failed to produce superhard TMDs. In general, the focus of future studies should be on quenchable phases that show superhard tendencies, or for ways to stabilize non-quenchable phases (like OII-$TiO_2$), that show worthy properties. Note that while superhardness is a desirable property, the hardness of the TMD phases may be adequate for many applications. This, along with the refractory nature of the TMDs, at least for room-pressure stable phases, makes them valuable in many applications. The continued refractory nature of TMD phases synthesized at high pressures and temperatures is still largely uninvestigated and should be pursued.

*Розглянуто поведінку діоксидів перехідних металів $TiO_2$, $ZrO_2$ і $HfO_2$ при високому тиску і високій температурі. Зокрема, розглянута і раніше передвіщена, і виміряна твердість, яка могла вказувати на надтверду поведінку. Показано, що надтвердий стан не притаманний діоксидам перехідних металів, що знаходяться в умовах навколишнього середовища, або фазам, отриманим при високому тиску і/або високій температурі.*

***Ключові слова**: діоксиди перехідних металів, високий тиск, твердість, діоксид титану, діоксид цирконію, діоксид гафнію.*

*Рассмотрено поведение диоксидов переходных металлов $TiO_2$, $ZrO_2$ и $HfO_2$ при высоком давлении и высокой температуре. В частности, рассмотрена и ранее предсказанная, и измеренная твердость, которая могла указывать на сверхтвердое поведение. Показано, что сверхтвердое состояние не присуще диоксидам переходных металлов, находящимся в условиях окружающей среды, или фазам, полученным при высоком давлении и/или высокой температуре.*

***Ключевые слова**: диоксиды переходных металлов, высокое давление, твердость, диоксид титана, диоксид циркония, диоксид гафния.*

1. *Adams D. M., Leonard S., Russell D. R. et al.* X-ray diffraction study of hafnia under high pressure using synchrotron radiation // J. Phys. Chem. Solids. – 1991. – **52**, N 9– P. 1181–1186.
2. *Al-Khatatbeh Y., Lee K. K. M., Kiefer B.* High-pressure behavior of $TiO_2$ as determined by experiment and theory // Phys. Rev. B. – 2009. – **79**, art. 134114.
3. *Al-Khatatbeh Y., Lee K. K. M., Kiefer B.* Phase relations and hardness trends of $ZrO_2$ phases at high pressure // Ibid. – 2010. – **81**, art. 214102.
4. *Al-Khatatbeh Y., Lee K. K. M., Kiefer B*. Phase diagram up to 105 GPa and mechanical strength of $HfO_2$ // Ibid. – 2010. – **82**, art. 144106.
5. *Arashi H.* Presure-induced phase transformation of $HfO_2$ // J. Am. Ceram. Soc. – 1992. – **75**, N 4. – P. 844–847.
6. *Arashi H., Yagi T., Akimoto S. et al.* New high-pressure phase of $ZrO_2$ above 35 GPa // Phys. Rev. B. – 1990. – **41**, N 7. – P. 4309–4313.
7. *Arlt T., Bermejo M., Blanco M. A. et al.* High-pressure polymorphs of anatase $TiO_2$ // Ibid. – 2000. – **61**, N 21, art. 14414.

8. *Boysen H., Frey F.* Neutron powder investigation of the tetragonal to monoclinic phase transformation in undoped zirconia // Acta Crystallogr. B. – 1991. – **47**, N 6. – P. 881–886.
9. *Dekura H., Tsuchiya T., Kuwayama Y. et al.* Theoretical and experimental evidence for a new post-cotunnite phase of titanium dioxide with significant optical absorption // Phys. Rev. Lett. – 2011. – **107**, art. 045701.
10. *Desgreniers S., Lagarec K.* High-density $ZrO_2$ and $HfO_2$: crystalline structures and equation of state // Phys. Rev. B. – 1999. – **59**, N 13. – P. 8467–8472.
11. *Dewhurst J. K., Lowther J. E.* Highly coordinated metal dioxides in the cotunnite structure // Ibid. – 2001. – **64**, art. 014104.
12. *Ding Y., Chen M., Wu W.* Mechanical properties, hardness, and electronic structures of new post-cotunnite phase ($Fe_2P$-type) of $TiO_2$ // Physica B. – 2013. – **433**. – P. 48–54.
13. *Dubrovinskaia N. A., Dubrovinsky L. S., Ahuja R. et al.* Experimental and theoretical identification of a new high-pressure $TiO_2$ polymorph // Phys. Rev. Lett. – 2001. – **87**, N 27, art. 275501.
14. *Dubrovinsky L. S., Dubrovinskaia N. A., Swamy V. et al.* The hardest known oxide // Nature (London). – 2001. – **410**. – P. 653–654.
15. *Gerward L., Olsen J. S.* Post-rutile high-pressure phases in $TiO_2$ // J. Appl. Crystallogr. – 1997. – **30**. – P. 259–264.
16. *Haines J., Leger J. M., Atouf A*. Crystal structure and equation of state of cotunnite-type zirconia // J. Am. Ceram. Soc. – 1995. – **78**, N 2. – P. 445–448.
17. *Haines J., Leger J. M., Hull S. et al.* Characterization of the cotunnite-type phases of zirconia and hafnia by neutron diffraction and Raman spectroscopy // Ibid. – 1997. – **80**, N 7. – P. 1910–1914.
18. *Howard C. J., Hill R. J., Reichert B. E*. Structures of $ZrO_2$ polymorphs at room temperature by high-resolution neutron powder diffraction // Acta Crystallogr. B. – 1988. – **44**, N 2. – P. 116–120.
19. *Jaffe J. E., Bachorz R. A., Gutowski M*. Low-temperature polymorphs of $ZrO_2$ and $HfO_2$: a density-functional theory study // Phys. Rev. B. – 2005. – **72**, art. 144107.
20. *Jayaraman A., Wang S. Y., Sharma S. K.* Pressure-induced phase transformations in $HfO_2$ to 50 GPa studied by Raman spectroscopy // Ibid. – 1993. – **48**, N 13. – P. 9205–9211.
21. *Kang J., Lee E.-C., Chang K. J.* First-principles study of structural phase transformation of hafnia under pressure // Ibid. – 2003. – **68**, art. 054106.
22. *Kudoh Y., Takeda H., Arashi H.* In situ determination of crystal structure for high-pressure phase of $ZrO_2$ using a diamond anvil and single crystal X-ray diffraction method // Phys. Chem. Minerals. – 1986. – **13**, N 4. – P. 233–237.
23. *Leger J. M., Tomaszewski P. E., Atouf A. et al*. Pressure-induced structural phase transitions in zirconia under high pressure // Phys. Rev. B. – 1993. – **47**, N 21. – P. 14075–14083.
24. *Leger J. M., Tomaszewski P. E., Atouf A. et al.* Pressure-induced phase transtions and volume changes in $HfO_2$ up to 50 GPa // Ibid. – 1993. – **48**, N 1. – P. 93–98.
25. *Lowther J. E., Dewhurst J. K., Leger J. M. et al*. Relative stability of $ZrO_2$ and $HfO_2$ structural phases// Ibid. – 1999. – **60**, N 21. – P. 14485–14488.
26. *Luo W., Yang S. F., Wang Z. C. et al*. Structural phase transitions in brookite-type $TiO_2$ under high pressure // Solid State Commun. – 2005. – **133**. – P. 49–53.
27. *Mattesini M., de Almeida J. S., Dubrovinsky L. et al*. High-pressure and high-temperature synthesis of the cubic $TiO_2$ polymorph // Phys. Rev. B. – 2004. – **70**, art. 212101.
28. *Nishio-Hamane D., Shimizu A., Nakahira R. et al.* The stability and equation of state for the cotunnite phase of $TiO_2$ up to 70 GPa // Phys. Chem. Minerals. – 2009. – **37**, N 3. – P. 129–136.
29. *Ohtaka O., Andrault D., Bouvier P. et al*. Phase relations and equation of state of $ZrO_2$ to 100 GPa // J. Appl. Crystallogr. – 2005. – **38**. – P. 727–733.
30. *Ohtaka O., Fukui H., Funakoshi K. et al*. Phase relations and EOS of $ZrO_2$ and $HfO_2$ under high-temperature and high-pressure // High Press. Res. – 2002. – **22**. – P. 221–226.
31. *Ohtaka O., Fukui H., Kunisada T. et al.* Phase relations and equations of state of $ZrO_2$ under high temperature and high pressure // Phys. Rev. B. – 2001. – **63**, art. 174108.
32. *Ohtaka O., Fukui H., Kunisada T. et al*. Phase relations and volume changes of hafnia under high pressure and high temperature // J. Am. Ceram. Soc. – 2001. – **84**, N 6. – P. 1369–1373.
33. *Ohtaka O., Kume S., Ito E.* Stabillity field of cotunnite-type zirconia // J. Am. Ceram. Soc. – 1990. – **73**, N 3. – P. 744–745.
34. *Ohtaka O., Yamanaka T., Kume S. et al.* Structural analysis of orthorhombic hafnia by neutron powder diffraction // Ibid. – 1995. – **78**, N 1. – P. 233–237.

35. *Ohtaka O., Yamanaka T., Kume S. et al*. Stability of monoclinic and orthorhombic zirconia: Studies by high-pressure phase equilibria and calorimetry // Ibid. – 1991. – **74**, N 3. – P. 505–509.
36. *Ohtaka O., Yamanaka T., Yagi T.* New high-pressure and -temperature phase of $ZrO_2$ above 1000 °C at 20 GPa // Phys. Rev. B. – 1994. – **49**, N 14. – P. 9295–9298.
37. *Swamy V., Dubrovinskaia N. A., Dubrovinsky L. S*. Compressibility of baddeleyite-type $TiO_2$ from static compression to 40 GPa // J. Alloys Comp. – 2002. – **340**. – P. 46–48.
38. *Tang J., Kai M., Kobayashi Y. et al*. A high-pressure high-temperature X-ray study of phase relations and polymorphism of $HfO_2$ // Properties of Earth and Planetary Materials at High Pressure and Temperature. – Washington, DC, USA: American Geophysical Union, 1998.
39. *Terki R., Bertrand G., Aourag H. et al*. Structural and electronic properties of zirconia phases: a FP-LAPW investigations // Mater. Sci. Semicon. Process. – 2006. – **9**. – P. 1006–1013.
40. *Lyakhov A. O, Oganov A. R.* Evolutionary search for superhard materials: Methodology and applications to forms of carbon and $TiO_2$ // Phys. Rev. B. – 2011. – **84**, art. 092103.
41. Al-*Khatatbeh Y., Lee K.K.M., Kiefer B.* Compressibility of nanocrystalline $TiO_2$ anatase // Phys. Chem. C. – 2012. – **116**, N 40. – P. 21635–21639.
42. *Dewhurst J. K., Lowther J. E*. High-pressure structural phases of titanium dioxide // Phys. Rev. B. – 1996. – **54**, N 6. – P. R3673–3675.
43. *Dewhurst J. K., Lowther J. E*. Relative stability, structure, and elastic properties of several phases of pure zirconia // Ibid. – 1998. – **57**, N 2. – P. 741–747.
44. *Fadda G., Colombo L., Zanzotto G.* First-principles study of the structural and elastic properties of zirconia // Ibid. – 2009. – **79**, art. 214102.
45. *Hearne G. R., Zhao J., Dawe A. M. et al.* Effect of grain size on structural transitions in anatase $TiO_2$: a Raman spectroscopy study at high pressure // Ibid. – 2004. – **70**, art. 134102.
46. *Muscat J., Swamy V., Harrison N. M.* First-principles calculations of the phase stability of $TiO_2$ // Ibid. – 2002. – **65**, art. 224112.
47. *Swamy V., Muddle B. C.* Ultrastiff cubic $TiO_2$ identified via first-principles calculations // Phys. Rev. Lett. – 2007. – **98**, art. 035502.
48. *Wang Y., Zhao Y., Zhang J. et al*. In situ phase transition study of nano- and coarse-grained $TiO_2$ under high pressure/temperature conditions // J. Phys. Condens. Matter. – 2008. – **20**, art. 125224.
49. *Caravaca M. A., Mino J. C., Perez V. J. et al*. Ab initio study of the elastic properties of single and polycrystal $TiO_2$, $ZrO_2$ and $HfO_2$ in the cotunnite structure // Ibid. – 2009. – **21**, art. 015501.
50. *Chen X., Mao S. S.* Titanium dioxide nanomaterials: Synthesis, properties, modifications, and applications // Chem. Rev. – 2007. – **107**, N 7. – P. 2891–2959.
51. *Valden M., Lai X., Goodman D. W.* Onset of catalytic activity of gold clusters on titania with the appearance of nonmetallic properties // Science. – 1998. – **281**. – P. 1647–1650.
52. *Lee W. E., Rainforth W. M.* Ceramic Microstructures: Property Control by Processing. – 1 ed. – London: Champan and Hall, 1994.
53. *Patil K. C., Hegde M. S. Rattan T. et al*. Ceramic Microstructures: Property Control by Processing. – Singapore: World Scientific Publishing Company, 2008.
54. *Fiorentini V., Gulleri G.* Theoretical evaluation of zirconia and hafnia as gate oxides for Si microelectronics // Phys. Rev. Lett. – 2002. – **89**, art. 266101.
55. *Griffin K. A. Pakhomov A. B. Wang C. M. et al.* Intrinsic ferromagnetism in insulating cobalt doped anatase $TiO_2$ // Ibid. – 2005. – **94**, art. 157204.
56. *Leinenweber K., Mosenfelder J., Diedrich T. et al.* High-pressure cells for in situ multi-anvil experiments // High Press. Res. – 2006. – **26**, N 3. – P. 283–292.
57. *Mergia K., Liedtke V., Speliotis T. et al.* Thermo-mechanical behaviour of $HfO_2$ coatings for aerospace applications // Adv. Mater. Res. – 2009. – **59**. – P. 87–91.
58. *Jiang X., Zhao J., Jiang X.* Correlation between hardness and elastic moduli of the covalent crystals // Comput. Mater. Sci. – 2011. – **50**, N 7. – P. 2287–2290.
59. *Mirgorodsky A. P., Quintard P. E.* Lattice-dynamic treatment of vibrational and elastic properties of cotunnite-type $ZrO_2$ and $HfO_2$: comparison with ambient pressure polymorphs // J. Am. Ceram. Soc. – 1999. – **82**, N 11. – P. 3121–3124.
60. *Liu Q., Liu Z., Feng L. et al*. First-principles study of structural, optical, and elastic properties of cubic $HfO_2$ // Physica B. – 2009. – **404**, N 20. – P. 3614–3619.
61. *Wilk G. D., Wallace R. M., Anthony J. M.* High-k gate dielectrics: current status and materials properties considerations // Phys. Rev. – 2001. – **89**, N 10. – P. 5243–5275.

62. *Lowther J. E.* Superhard ceramic oxides // MRS Bull. – 2003. – **28**, N 3. – P. 189–193.
63. *Öztürk H., Durandurdu M.* High-pressure phases of $ZrO_2$: an *ab initio* constant-pressure study // Phys. Rev. B. – 2009. – **79**, art. 134111.
64. *Teter D. M.* Computational alchemy: The search for new superhard materials // MRS Bull. – 1998. – **23**, N 1. – P. 22–27.
65. *Haines J., Leger J. M., Bocquillon G.* Synthesis and design of superhard materials // Annu. Rev. Mater. Res. – 2001. – **31**, N 1. – P. 1–23.
66. *Brazhkin V. V., Lyapin A. G., Hemley R. J.* Harder than diamond: dreams and reality // Phill. Mag. A. – 2002. – **82**, N 2. – P. 231–253.
67. *Haines J., Leger J. M., Schmidt M. et al.* The search for new superhard materials // Proc. XXXIV EHPRG Conf., Leuven, Belgium: Leuven University Press, 1997.
68. *Takai O.* Superhard Materials // Novel Concepts to Develop Carbon Science and Technology / Eds. E. Yasuda et al. – Oxford: Elsevier Science Ltd., 2003.
69. *Holleck H.* Material selection for hard coatings // J. Vac. Sci. Tech. A. – 1986. – **4**, N 6. – P. 2661–2669.
70. *Chan S.-K., Fang Y., Grimsditch M. H. et al.* Temperature dependence of the elastic moduli of monoclinic zirconia // J. Am. Ceram. Soc. – 1991. – **74**, N 7. – P. 1742–1744.
71. *Nevit, M. V., Chan S.-K., Liu J. Z. et al.* The elastic properties of monoclinic $ZrO_2$, Physica B. – 1988. – **150**. – P. 230–233.
72. *Anderson O. L.* The use of ultrasonic measurements under modest pressure to estimate compression at high pressure // J. Phys. Chem. Solids. – 1966. – **27**. – P. 547–565.
73. *Birch F.* Elasticity and constitution of the Earth's interior // J. Geophys. Res. – 1952. – **57**. – P. 227–234.
74. *Jeanloz R.* Universal equation of state // Phys. Rev. B. – 1988. – **38**, N 1. – P. 805–807.
75. *Jeanloz R.* Finite-strain equation of state for high-pressure phases // Geophys. Res. Lett. – 1981. – **8**, N 12. – P. 1219–1222.
76. *Birch F.* Finite strain isotherm and velocities for single-crystal and polycrystalline NaCl at high pressures and 300 K // J. Geophys. Res. – 1978. – **83**. – P. 1257–1268.
77. *Chung H.-Y., Weinberger M. B., Levine J. B. et al.* Synthesis of ultra-incompressible superhard rhenium diboride at ambient pressure // Science. – 2007. – **316**, N 5823. – P. 436–439.
78. *Bulter J. E., Windischmann H.* Developments in CVD-diamond synthesis during the past decade // MRS Bull. – 1998. – **23**, N 9. – P. 22–27.
79. *Wang Y., Panzik J. E., Kiefer B. et al.* Crystal structure of graphite under room-temperature compression and decompression // Sci. Reports. – 2012. – **2**, art. 520.
80. *Zerr A., Miehe G., Serghiou G. et al.* Synthesis of cubic silicon nitride // Nature (London). – 1999. – **400**. – P. 340–342.
81. *Wang Y., Lee K.K.M.* From soft to superhard: fifty years of experiments on cold compressed graphite // J. Superhard Mater. – 2012. – **34**, N 6. – P. 360–370.
82. *Hu J. Z., Mao H. K., Shu J. F. et al.* Diamond anvil cell radial X-ray diffraction program at the National Synchrotron Light Source // J. Phys. Condens. Matter. – 2006. – **18**. – P. S1091–S1096.
83. *Jiang J. Z., Lindelov H., Gerward L. et al.* Compressibility and thermal expansion of cubic silicon nitride // Phys. Rev. B. – 2002. – **65**, art. 161202(R).
84. *Quintard P. E., Barberis P., Mirgorodsky A. P. et al.* Comparative lattice-dynamical study of the Raman spectra of monoclinic and tetragonal phases of zirconia and hafnia // J. Am. Ceram. Soc. – 2002. – **85**, N 7. – P. 1745–1749.
85. *Teufer G.* The crystal structure of tetragonal $ZrO_2$ // Acta Crystallogr. – 1962. – **15**. – P. 1187–1189.
86. *Smith D. K., Cline C. F.* Verification of existence of cubic zirconia at high temperature // J. Am. Ceram. Soc. – 1962. – **45**. – P. 249–250.
87. *Wang J., Li H. P., Stevens R.* Hafnia and hafnia-toughened ceramics // J. Mater. Sci. – 1992. – **27**, N 20. – P. 5397–5430.
88. *Ohtaka O., Yamanaka T., Kume S. et al.* Structural analysis of orthorhombic $ZrO_2$ by high resolution neutron powder diffraction // Proc. Japan Acad. B. – 1990. – **66**. – P. 193–196.
89. *Ohtaka O., Yamanaka T., Kume S. et al.* Synthesis and X-ray structural analysis by the Rietveld method of orthorhombic hafnia // J. Ceram. Soc. Japan. – 1991. – **99**. – P. 826–827.
90. *Kourouklis G. A., Liarokapis E.* Pressure and temperature dependence of the Raman spectra of zirconia and hafnia // J. Am. Ceram. Soc. – 1991. – **74**, N 3. – P. 520–523.

91. *Shul'ga Y. M., Matyushenko D. V., Golyshev A. A. et al*. Phase transformations in nanostructural anatase $TiO_2$ under shock compression conditions studied by Raman spectroscopy // Tech. Phys. Lett. – 2010. – **36**, N 9. – P. 841–843.
92. *Swamy V., Kuznetsov A., Dubrovinsky L. S. et al*. Finite-size and pressure effects on the Raman spectrum of nanocrystalline anatase $TiO_2$ // Phys. Rev. B. – 2005. – **71**, art. 184302.
93. *Wang Z., Saxena S. K.* Raman spectroscopic study on pressure-induced amorphization in nanocrystalline anatase ($TiO_2$) // Solid State Commun. – 2001. – **118**. – P. 75–78.
94. *Haines J., Leger J. M., Schulte O*. The high-pressure phase transition sequence from the rutile-type through to the cotunnite-type structure in $PbO_2$ // J. Phys. Condens. Matter. – 1996. – **8**. – P. 1631–1646.
95. *Hazen R. M., Finger L. W*. Bulk moduli and high-pressure crystal structures of rutile-type compounds // J. Phys. Chem. Solids. – 1981. – **42**. – P. 143–151.
96. *Simunek A., Vackar J*. Hardness of covalent and ionic crystals: First-principle calculations // Phys. Rev. Lett. – 2006. – **96**, art. 085501.

Department of Basic Sciences,
Princess Sumaya University for Technology
Department of Geology and Geophysics,
Yale University

Received 15.03.14